

# Insight into gain and transient response characteristics of AlGaIn/GaN hetero-junction based UV photodetectors: Case study on the role of incident light intensity

Cite as: Appl. Phys. Lett. **125**, 231104 (2024); doi: 10.1063/5.0227700

Submitted: 10 July 2024 · Accepted: 3 October 2024 ·

Published Online: 3 December 2024



Wenxin Li,<sup>1</sup> Yifu Wang,<sup>1</sup> Guangyang Gu,<sup>1</sup> Fangfang Ren,<sup>1,2</sup> Dong Zhou,<sup>1</sup> Weizong Xu,<sup>1,2,a)</sup> Feng Zhou,<sup>1</sup> Dunjun Chen,<sup>1</sup> Rong Zhang,<sup>1,2</sup> Youdou Zheng,<sup>1</sup> and Hai Lu<sup>1,2,3,a)</sup>

## AFFILIATIONS

<sup>1</sup>School of Electronic Science and Engineering, Nanjing University, Nanjing 210093, China

<sup>2</sup>Hefei National Laboratory, Hefei 230088, China

<sup>3</sup>The Key Lab of Optoelectronic Devices and Systems with Extreme Performances, MOE, 210023, China

<sup>a)</sup>Authors to whom correspondence should be addressed: [wz.xu@nju.edu.cn](mailto:wz.xu@nju.edu.cn) and [hailu@nju.edu.cn](mailto:hailu@nju.edu.cn)

## ABSTRACT

Gain and response speed are two key performance parameters for high sensitivity photodetectors (PDs). However, the effect of incident light intensity on gain and transient response properties of AlGaIn/GaN hetero-junction based PDs are still not fully understood. Here, we design and fabricate an AlGaIn/GaN hetero-junction based ultraviolet (UV) PD with interdigitated electrodes formed by a conductive two-dimensional electron gas (2DEG) channel, which exhibits a low dark current of  $2.92 \times 10^{-11}$  A and a high responsivity of 3060 A/W at 10 V bias. The high-gain AlGaIn/GaN 2DEG PD has a similar working mechanism to those of traditional phototransistors, but its device architecture is evidently simplified. By investigating the variation of gain and transient response characteristics of the 2DEG PD as a function of incident UV light intensity, it has been concluded that the gain of the PD in a low-light intensity region is dominated by hole accumulation-induced electron escape from the 2DEG, while in a high-light intensity region, the gain is dominated by photoconductivity effect and limited by carrier recombination. This study provides guidance for future practical applications of AlGaIn/GaN-based PDs in complex UV illumination environments.

Published under an exclusive license by AIP Publishing. <https://doi.org/10.1063/5.0227700>

As a wide bandgap semiconductor with numerous excellent physical properties, GaN is an ideal material for fabricating high-performance ultraviolet photodetectors (UV PDs).<sup>1–3</sup> In specific application scenarios requiring high detection sensitivity, a desired UV PD should possess high gain and fast response speed simultaneously. Meanwhile, low-voltage operation is also preferred.<sup>4</sup> The AlGaIn/GaN heterostructure with a strong polarization effect has been widely studied to build the high-responsivity UV PDs owing to the presence of high-mobility and high-concentration two-dimensional electron gas (2DEG) at the AlGaIn/GaN heterointerface.<sup>5–7</sup> Although the 2DEG conductive channel could bring high responsivity of the PDs, it may also lead to high dark current.<sup>8,9</sup> Currently, approaches to solve this issue are mainly to create an additional gate control on the AlGaIn/GaN hetero-junction (such as p-GaN cap layer<sup>10,11</sup> and semi-transparent metal gate,<sup>12,13</sup> etc.), which can deplete the 2DEG channel

under dark condition and also modulate the channel conductivity under UV illumination. In this way, these modified PDs work as phototransistors based on photogating effect.<sup>14–16</sup> Because of the above mechanism, the gain of these PDs is usually not a constant and could change significantly as a function of incident light intensity.<sup>17</sup> At present, research interest is mainly focused on achieving higher device gain in AlGaIn/GaN hetero-junction based PDs.<sup>18–20</sup> Nevertheless, there is still a lack of in-depth understanding of the gain mechanisms at different light illumination intensities. In addition, there is no consistent illumination condition to measure the response speed of these high-gain devices, which should have a strong correlation with the device gain as well.

In this work, we design and fabricate an AlGaIn/GaN hetero-junction based PD with interdigitated mesa electrodes formed by 2DEG, which possesses low dark current and high responsivity. The

low dark current is achieved with the interruption of the 2DEG conductive channel by recess isolation, while the high gain can be attributed to hole accumulation-induced escape of electrons from the 2DEG channel into the conduction band. This PD has a similar operation mechanism to those of traditional phototransistors, but owns a simplified device architecture. By exploring the evolution of gain and transient response speed as a function of incident UV light intensity, the dominant gain mechanism of this high-gain PD is revealed, which explains the correlation behaviors between gain and response speed.

The AlGaIn/GaN hetero-junction based PD is fabricated on commercial GaN-on-sapphire wafer grown by metal-organic chemical vapor deposition. The epi-structure consists of a  $1\text{ }\mu\text{m}$  AlN buffer layer, a  $300\text{ nm}$  undoped GaN channel layer, a  $1\text{ nm}$  AlN spacer layer, and a  $20\text{ nm}$   $\text{Al}_{0.25}\text{Ga}_{0.75}\text{N}$  barrier layer. Its room-temperature 2DEG density and electron mobility are  $1.5 \times 10^{13}\text{ cm}^{-2}$  and  $1400\text{ cm}^2/\text{Vs}$ , respectively. The schematic diagram of the PD is shown in Fig. 1(a), which is based on 2DEG interdigitated mesa electrodes with a width of  $5\text{ }\mu\text{m}$  separated by a  $5\text{ }\mu\text{m}$  gap. The isolation gap between the two mesa fingers is realized by dry etching down to the undoped GaN layer with a depth of  $\sim 55\text{ nm}$ . After the mesa formation, ohmic contact metal consisting of a Ti( $20\text{ nm}$ )/Al( $135\text{ nm}$ )/Ni( $50\text{ nm}$ )/Au( $45\text{ nm}$ ) stack is deposited by electron beam evaporation and patterned by a lift-off technique, which is followed by rapid-thermal annealing at  $850^\circ\text{C}$  for  $1\text{ min}$  in  $\text{N}_2$  atmosphere. The specific contact resistivity ( $\rho_c$ ) between the AlGaIn/GaN heterostructure and the alloying metal has been calculated to  $3.51 \times 10^{-4}\text{ }\Omega\text{ cm}^2$  by the method of transmission line model (TLM), indicating that the excellent ohmic contact has been formed in the fabricated PD (a detailed discussion can be found in the [supplementary material](#), Sec. 1). Next, a Ti( $300\text{ nm}$ )/Au( $700\text{ nm}$ ) metal pad layer is deposited to facilitate wire bonding and electrical testing. Finally, the PD is passivated by a  $10\text{ nm}$   $\text{Al}_2\text{O}_3$  film deposited by atomic layer deposition. A top-view image of one fabricated PD is shown in Fig. 1(b).

Compared with traditional metal–semiconductor–metal structures,<sup>21</sup> this PD utilizes 2DEG mesa electrodes instead of metal electrodes for photo-carrier collection, which not only reduces the metal contact related shading effect but also has a different carrier drift mechanism. As shown in Fig. 1(c), the electric field distribution of the 2DEG PD under dark condition is simulated by employing Silvaco TCAD software. The electrical field strength is obviously stronger near the 2DEG channel, which drops and extends along the highly resistive GaN gap. The enhanced electrical field is caused by the energy barrier between the 2DEG channel and the underlying GaN. In this case, the 2DEG channel acts like a “Schottky metal,” which partly limits the dark current flow under reverse bias. Under UV illumination, electron and hole pairs are generated within the GaN channel layer and drift toward anode and cathode under a lateral electric field, respectively. Because of the AlGaIn energy barrier, some holes would trap and accumulate at the AlGaIn/GaN interface at the cathode side of the new device structure, which would induce additional electron injection from the 2DEG channel into the GaN channel to maintain the charge neutrality condition [see Fig. 1(d)]. This new electron injection mechanism would lead to a higher photocurrent and large device gain.

The current–voltage (I–V) characteristics of the AlGaIn/GaN 2DEG PD under dark and  $365\text{ nm}$  illumination were performed by using a Keithley 2636B source meter. As shown in Fig. 2(a), the PD exhibits a low dark current of  $\sim 2.92 \times 10^{-11}\text{ A}$  at  $10\text{ V}$  bias, indicating that the undoped GaN isolation layer can effectively cut off the 2DEG channel. The PD also exhibits good UV sensitivity and large photo-to-dark current ratio (PDCR) under low bias. Under a weak UV illumination condition of  $\sim 5\text{ }\mu\text{W}/\text{cm}^2$ , a high photocurrent of  $1.87 \times 10^{-5}\text{ A}$  and a corresponding PDCR of more than  $10^6$  can be achieved at  $10\text{ V}$  bias. The photoresponse curves of the PD were measured by using a Xe lamp equipped with an iHR320 monochromator for single wavelength light selection. As displayed in Fig. 2(b), the peak responsivity occurs at  $\sim 365\text{ nm}$ , corresponding to the bandgap energy of GaN.

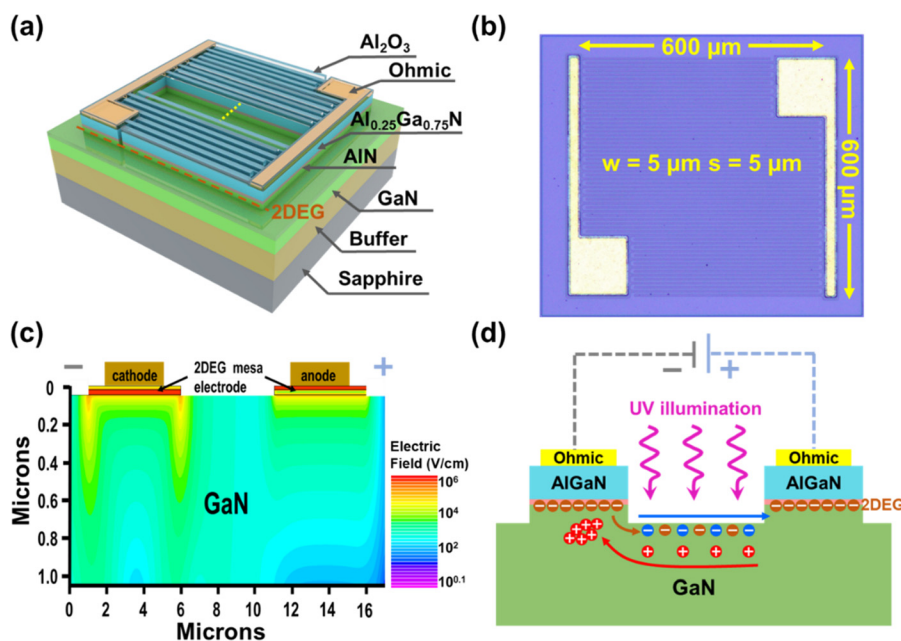


**FIG. 1.** (a) The schematic diagram and (b) the top-view microscopy image of the fabricated AlGaIn/GaN 2DEG PD. (c) Simulated 2D electric field distribution profile at  $10\text{ V}$  bias under dark condition, and (d) schematic cross-sectional view of the illustrated drift path of the photogenerated carriers and illumination-induced carriers under light illumination.

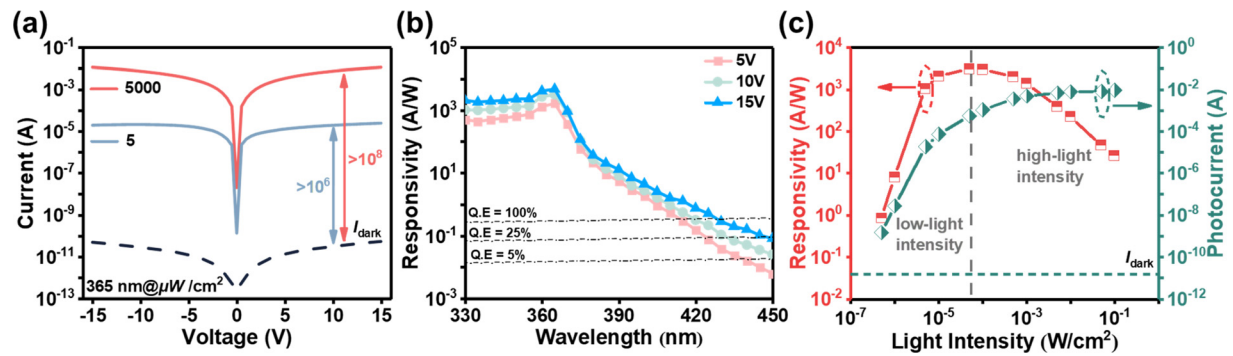


**FIG. 2.** (a) I–V characteristics of the AlGaIn/GaN 2DEG PD under the dark and 365-nm LED illumination with 5 and 5000  $\mu\text{W}/\text{cm}^2$  light intensity. (b) The photoresponse spectra under different biases. (c) The photocurrent and responsivity at 10 V as a function of the intensities of 365-nm UV illumination from 0.5  $\mu\text{W}/\text{cm}^2$  to 100  $\text{mW}/\text{cm}^2$ .

The UV/visible (365/400 nm) rejection ratio is more than three orders of magnitude. The overall photoresponse of the PD also increases considerably with the increase in applied bias, indicating that the electrical field has a big impact on the device gain.

To further investigate the internal gain mechanisms, the photocurrent and responsivity of the AlGaIn/GaN 2DEG PD are measured as a function of the UV illumination intensity. As shown in Fig. 2(c), when the UV intensity increases from 0.5 to 50  $\mu\text{W}/\text{cm}^2$  (defined as low-light intensity region), both the device photocurrent and its responsivity rise rapidly. Specifically, the responsivity increases from  $\sim 1$  A/W to a peak value of  $\sim 3060$  A/W, which is higher than those of most traditional metal–semiconductor–metal PDs.<sup>21,22</sup> When the UV intensity is above 50  $\mu\text{W}/\text{cm}^2$  (defined as high-light intensity region), the photocurrent tends to saturate and the corresponding responsivity drops to 25.8 A/W at 100  $\text{mW}/\text{cm}^2$ . The observed evolution behavior of the responsivity is similar to those of the previously reported high-gain III-nitride-based phototransistors.<sup>12</sup> Thus, there might be different mechanisms limiting the maximum gain of the PD at different light illumination levels. Meanwhile, in order to evaluate the effect of electrode spacing on the device gain, the responsivity of diverse 2DEG PDs with different electrode spacing (2–15  $\mu\text{m}$ ) are also measured as a function of the UV illumination intensity (detailed discussion can be found in the [supplementary material](#), Sec. 2).

Since the gain mechanism largely determines the transient response speed, the transient response characteristic could be utilized as the criterion in the investigation of the gain mechanism. In this work, the transient response characteristics of the PD is measured by using the setup shown in Fig. 3, where a 365 nm LED driven by a high-speed pulse width modulator (PWM) is used to provide square-wave UV light. The magnitude of the square signals is adjusted by the LED on-current and a series of neutral density (ND) filters. A high-speed transimpedance amplifier circuit is used to measure the transient response current from the PD. The system time delay evaluated by using a high-speed Si photodiode is found below 1  $\mu\text{s}$  for the whole test setup. Compared with the traditional method that the PD is directly connected in series with a resistor to obtain transient waveform, the advantage of this setup is that the bias on the PD could be clamped during transient test. Thereby, the influence of transient bias change on the PD gain is negligible, which is important in studying the real transient response characteristics related to the gain mechanism.

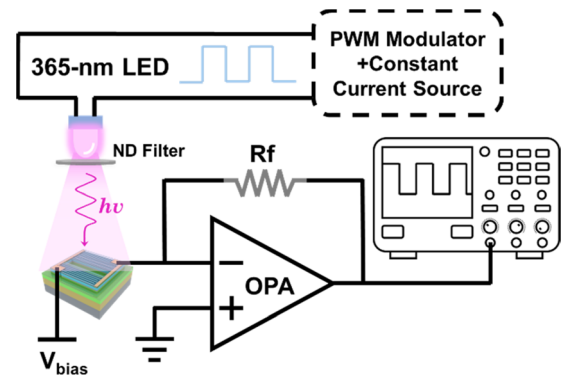


**FIG. 3.** Schematic of the test platform for the AlGaIn/GaN 2DEG PD transient response characterization.

The acquired transient response waveforms of the AlGaIn/GaN 2DEG PD in low- and high-light intensity regions are shown in Figs. 4(a) and 4(b), respectively. The rise ( $t_r$ ) and decay ( $t_d$ ) times, extracted from the normalized transient response curves [see inset of Figs. 4(a) and 4(b)], are defined as the time for the signal to rise from 10% to 90% or drop from 90% to 10% of the corresponding full amplitude. The results are plotted as a function of light intensity as illustrated in Figs. 4(c) and 4(d). It can be clearly seen that the response speed of the PD becomes faster as the light intensity increases. Generally, the larger the device gain, the slower the response speed.<sup>23</sup> In a high-light intensity region, the relationship between the gain and response speed of the device is consistent with the above rule. However, in a low-light intensity region, as has been shown in Fig. 2(c) that the device gain increases as a function of light intensity, it is found that the response speed of the PD also becomes faster simultaneously. This observation is against the general rule mentioned above, which confirms that the 2DEG PD has a different gain mechanism in a low-light intensity region compared with that in a high-light intensity region.

In view of the ohmic contact nature of the two electrodes, a photoconductive gain should always exist within the device as electrons drift much faster than holes. However, based on the following two reasons, only photoconductive gain is insufficient to explain the

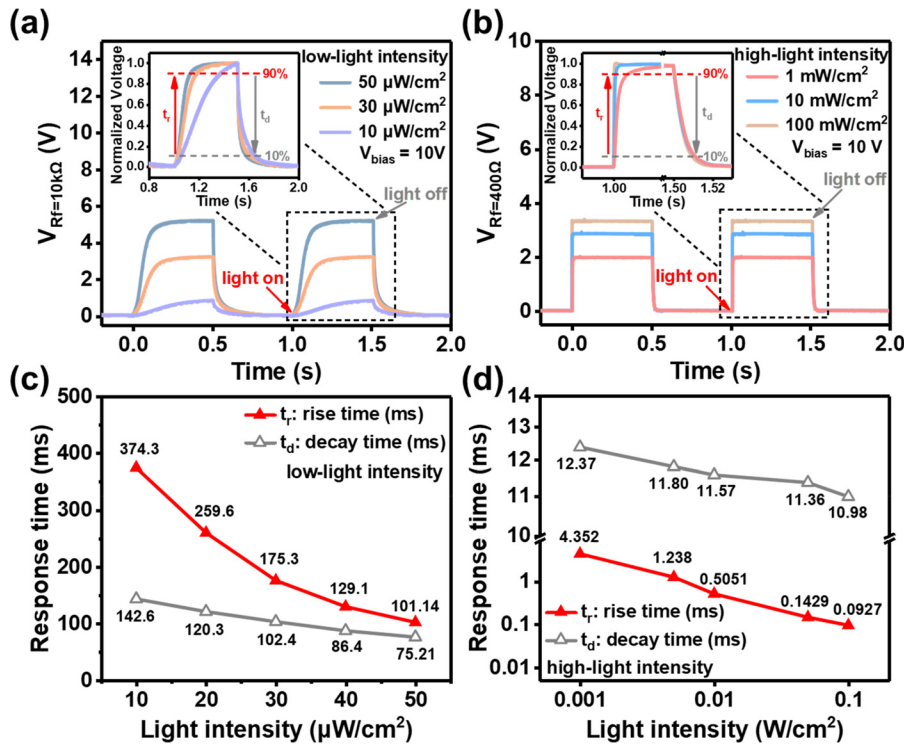


FIG. 4. Transient response of the AlGaIn/GaN 2DEG PD at 10 V in (a) low- and (b) high-light intensity regions (the insets show the normalized response for one single cycle). The rise and decay times in (c) low- and (d) high-light intensity regions as a function of the light intensity.

performance of the AlGaIn/GaN 2DEG PD. First, as previously reported, a standard gain model of photoconductors has been used to explain the gain mechanism of an InAlN/GaN hetero-junction based PD with a similar structure to this work.<sup>24</sup> In the model, the photoconductive gain can be expressed by the following formula:  $G = \tau_r \mu_e V / W^2$ , where  $W$  is the spacing between electrodes,  $\tau_r$  is the recombination time,  $\mu_e$  is the electron mobility, and  $V$  is the bias voltage. Assuming that the electron mobility of the undoped GaN channel layer of the PD in this work is  $300 \text{ cm}^2/\text{V s}$ , if the above simple photoconductive gain model is applied to explain the obtained maximum gain of the 2DEG PD, a recombination time as large as  $0.8 \mu\text{s}$  would be deduced, which is unrealistically larger than the earlier reported minority carrier lifetime of hetero-epitaxial GaN. Second, it is well known that the photoconductive gain of a PD would generally decrease with the increase in incident light intensity. It is because those high density photo-carriers would screen the electrical field within the device channel, which would weaken the separation efficiency of electron-hole pairs and then lead to enhanced recombination. Nevertheless, as shown in Fig. 2(c), the device gain increases as a function of incident light intensity in a low-light intensity region.

In view of the above gain and response speed behaviors, an additional gain mechanism is purposed and schematically illustrated with the band structure diagram in Fig. 5(a). Under the excitation of UV illumination, electron-hole pairs are generated within the GaN channel and then drift toward opposite directions under the influence of an electric field. Because of the energy barrier existing at the AlGaIn/GaN interface, excess holes would accumulate at the interface, resulting in an electrostatic reduction of the energy barrier height for electrons in the quantum well [dotted line in Fig. 5(a)]. This creates conditions for

electrons in 2DEG to escape from the quantum well into the GaN conduction band, thereby bringing an additional gain to the 2DEG PD. The variation of carrier density ( $\Delta n_e$ ) in the GaN channel due to the escape of electrons can be estimated as

$$\Delta n_e \approx \frac{k_b T m^*}{\pi \hbar^2} \exp \left[ -\frac{q(\phi_b - \Delta\phi)}{k_b T} \right], \quad (1)$$

where  $\phi_b$  is the energy separation between the Fermi level and the bottom of GaN conduction band,  $\Delta\phi$  is the reduction of barrier height caused by the hole accumulation,  $k_b$  is the Boltzmann constant,  $m^*$  is the effective mass of electron, and  $\hbar$  is the Planck constant. Assuming all escaped electrons can finally reach the other electrode without recombination during the drift, the gain ( $G_{\Delta n}$ ) due to the carrier concentration change can be expressed as

$$G_{\Delta n} = \frac{\Delta n_e \mu_e V}{f_{ph} W^2}, \quad (2)$$

where  $f_{ph}$  is the photo flux per unit area. Given the fact that the responsivity of the 2DEG PD increases dramatically with the enhanced light intensity in a low-light intensity region,  $\Delta n_e$  with exponential property should be the dominant factor in Eq. (2), which surpasses the influence of  $f_{ph}$  in the denominator. Therefore, device gain in a low-light intensity region should be dominated by hole accumulation-induced barrier lowering and electron escape rather than photoconductive gain. As light intensity further increases,  $\Delta\phi$  caused by hole accumulation would tend to reach a saturation point  $\phi_s$ , which is caused by the enhanced carrier recombination at the AlGaIn/GaN interface. As a result,  $\Delta n_e$  also tends to saturate and cannot bring a higher gain to the



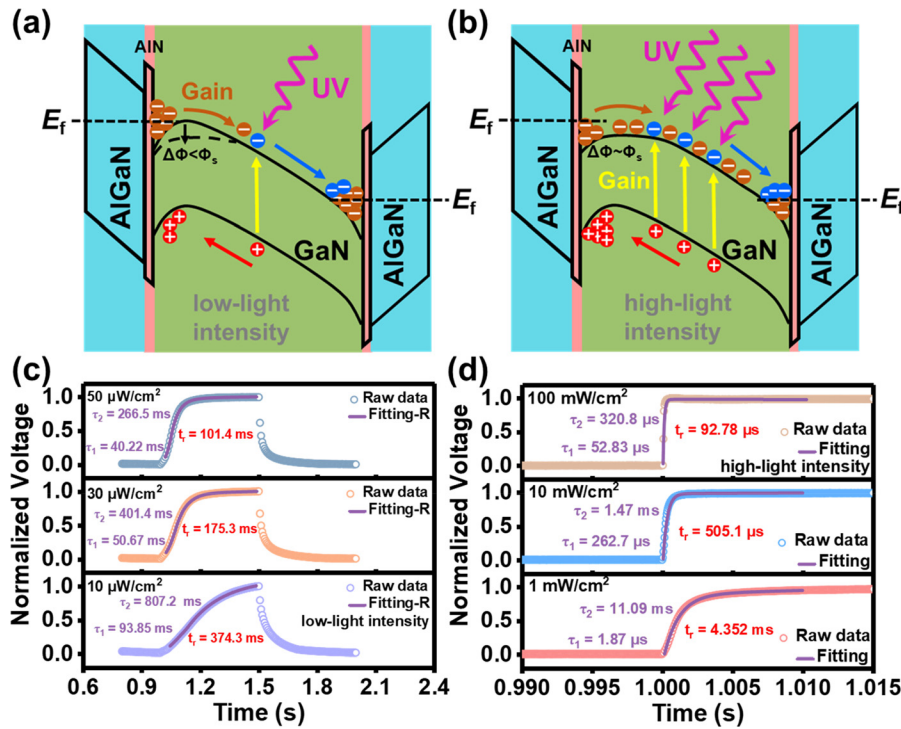


FIG. 5. Schematic band diagrams of the AlGaIn/GaN 2DEG PD in (a) low- and (b) high-light intensity regions (where  $\Delta\Phi$  and  $\Phi_s$ , respectively, denote the barrier reduction and the saturation point of the barrier reduction due to the hole accumulation). Normalized transient response curves and fitted curves of the rise processes in (c) low- and (d) high-light intensity regions for the 2DEG PD.

PD. Meanwhile, due to the enhanced carrier recombination in the GaN channel, the photoconductive gain of the PD would decrease at higher light illumination intensity, which is consistent with the actual result shown in Fig. 2(c). Thus, the device gain in a high-light intensity region should be governed by photoconductive gain as illustrated in Fig. 5(b).

To further understand the purposed gain mechanisms of the AlGaIn/GaN 2DEG PD at different light intensities, the rise edges of the normalized transient response curves are fitted by the following biexponential relaxation function:<sup>25,26</sup>

$$V(t) = \left( I_{\text{dark}} + Ae^{\frac{-t}{\tau_1}} + Be^{\frac{-t}{\tau_2}} \right) R_F, \quad (3)$$

where  $I_{\text{dark}}$  is the initial dark current,  $R_F$  is the feedback resistor,  $\tau_1$  and  $\tau_2$  are relaxation time constants for fast and slow rise components, respectively. The fast rise component is governed by minority carrier recombination, while the slow rise component is determined by emission lifetime of trapped carriers. For the case of the 2DEG PD, trapped carriers mainly refer to electrons in the 2DEG quantum well. As shown in Figs. 5(c) and 5(d), the contributions of  $\tau_1$  and  $\tau_2$  to the response time ( $t_r$ ) can be deduced at different light illumination intensities. In a low-light intensity region, it is found that the slow rise component ( $\tau_2$ ) is the dominant factor for  $t_r$ , which agrees with the purposed gain mechanism of hole accumulation-induced electron escape from the quantum well. Moreover,  $\tau_2$  gradually decreases as light intensity increases, which can be attributed to the fact that larger barrier height reduction makes it easier for electrons to escape. However, in a high-light intensity region, it is found that the fast rise component ( $\tau_1$ ) dominates  $t_r$ . This observation indicates that the photoresponse is highly dependent on carrier recombination, thus verifying that the

photoconductivity effect governs the device gain at high-light intensities. Furthermore, as light intensity increases, both gain and  $\tau_1$  decrease due to enhanced carrier recombination, resulting in a faster response speed of the 2DEG PD. Thus, based on the above response speed analysis, the suggested gain mechanisms of the 2DEG PD at different light illumination conditions are confirmed.

In summary, an AlGaIn/GaN hetero-junction based PD with high responsivity is designed and fabricated. The proposed working mechanism of the PD is similar to those of traditional phototransistors, in which its high gain is caused by hole-accumulation-induced barrier lowering and escape of electrons from 2DEG. By studying the variation of gain and transient response characteristics of the PD as a function of incident UV light, the gain mechanisms in low-to-high illumination conditions are confirmed. In addition, this study also reveals the reason why some high-gain type PDs in the literature can exhibit very fast response under strong pulsed laser illumination. This is because their method of acquiring a fast response speed is accompanied by sacrificing device gain, the obtained response speed is not the true response speed of the PDs at their highest gain.

See the [supplementary material](#) for details on the characterization of the ohmic contact and a supplementary discussion on the effect of electrode spacing for the device gain.

This work was supported in part by the Innovation Program for Quantum Science and Technology under Grant No. 2021ZD0303400; in part by the Key Research Program of Jiangsu Province under Grant No. BE2023018; in part by the National Nature Science Foundation of China under Grant Nos. 61921005, U2141241, 62374084, and U21A20496; in part by funding from the

Science and Technology on Monolithic Integrated Circuits and Modules Laboratory under Grant No. 61428032201; and in part by the National Key Research and Development Program of China under Grant No. 2022YFB3604900 and the Fundamental Research Funds for the Central Universities.

## AUTHOR DECLARATIONS

### Conflict of Interest

The authors have no conflicts to disclose.

### Author Contributions

**Wenxin Li:** Conceptualization (lead); Data curation (lead); Formal analysis (lead); Investigation (lead); Methodology (lead); Software (lead); Visualization (lead); Writing – original draft (lead). **Yifu Wang:** Data curation (supporting); Formal analysis (supporting); Investigation (supporting); Validation (supporting). **Guangyang Gu:** Formal analysis (supporting); Investigation (supporting); Software (equal). **Fangfang Ren:** Funding acquisition (equal); Investigation (supporting); Supervision (equal). **Dong Zhou:** Formal analysis (supporting); Investigation (supporting); Resources (supporting). **Weizong Xu:** Conceptualization (supporting); Data curation (supporting); Funding acquisition (equal); Investigation (equal); Methodology (equal); Supervision (equal); Visualization (supporting); Writing – review & editing (equal). **Feng Zhou:** Formal analysis (supporting); Writing – review & editing (supporting). **Dunjun Chen:** Funding acquisition (supporting); Investigation (supporting). **Rong Zhang:** Funding acquisition (equal); Investigation (supporting); Resources (equal); Supervision (supporting). **Youdou Zheng:** Conceptualization (supporting); Project administration (supporting); Supervision (equal). **Hai Lu:** Conceptualization (lead); Data curation (equal); Formal analysis (equal); Funding acquisition (lead); Investigation (equal); Methodology (equal); Project administration (lead); Resources (equal); Supervision (lead); Writing – original draft (lead); Writing – review & editing (lead).

### DATA AVAILABILITY

The data that support the findings of this study are available from the corresponding authors upon reasonable request.

## REFERENCES

- <sup>1</sup>E. Monroy, F. Omnès, and F. Calle, *Semicond. Sci. Technol.* **18**(4), R33–R51 (2003).
- <sup>2</sup>E. Muñoz, *Phys. Status Solidi B* **244**(8), 2859–2877 (2007).
- <sup>3</sup>Y. Tsai, K. Lai, M. Lee, Y. Liao, B. S. Ooi, H. Kuo, and J. He, *Prog. Quant. Electron.* **49**, 1–25 (2016).
- <sup>4</sup>B. Pandit, H. S. Jang, Y. Jeong, S. An, S. Chandramohan, K. K. Min, S. M. Won, C. J. Choi, J. Cho, S. Hong, and K. Heo, *Adv. Mater. Interfaces* **10**(12), 2202379 (2023).
- <sup>5</sup>T. Kuan, S. Chang, Y. Su, C. Ko, J. B. Webb, J. A. Bardwell, Y. Liu, H. Tang, W. Lin, Y. Cherng, and W. Lan, *Jpn. J. Appl. Phys., Part 1* **42**, 5563–5564 (2003).
- <sup>6</sup>L. Li, D. Hosomi, Y. Miyachi, T. Hamada, M. Miyoshi, and T. Egawa, *Appl. Phys. Lett.* **111**(10), 102106 (2017).
- <sup>7</sup>B. Pandit, E. F. Schubert, and J. Cho, *Sci. Rep.* **10**(1), 22059 (2020).
- <sup>8</sup>H. Zhang, C. Huang, K. Song, H. Yu, C. Xing, D. Wang, Z. Liu, and H. Sun, *Rep. Prog. Phys.* **84**(4), 044401 (2021).
- <sup>9</sup>M. Martens, J. Schlegel, P. Vogt, F. Brunner, R. Lossy, J. Würfl, M. Weyers, and M. Kneissl, *Appl. Phys. Lett.* **98**(21), 211114 (2011).
- <sup>10</sup>Q. Lyu, H. Jiang, and K. M. Lau, *Appl. Phys. Lett.* **117**(7), 71101 (2020).
- <sup>11</sup>H. Wang, H. You, Y. Xu, X. Sun, Y. Wang, D. Pan, J. Ye, B. Liu, D. Chen, H. Lu, R. Zhang, and Y. Zheng, *ACS Photonics* **9**(6), 2040–2045 (2022).
- <sup>12</sup>H. Zhang, F. Liang, K. Song, C. Xing, D. Wang, H. Yu, C. Huang, Y. Sun, L. Yang, X. Zhao, H. Sun, and S. Long, *Appl. Phys. Lett.* **118**(24), 242105 (2021).
- <sup>13</sup>A. M. Armstrong, B. Klein, A. A. Allerman, E. A. Douglas, A. G. Baca, M. H. Crawford, G. W. Pickrell, and C. A. Sanchez, *J. Appl. Phys.* **123**(11), 114502 (2018).
- <sup>14</sup>S. Baek, G. Lee, C. Cho, and S. Lee, *Sci. Rep.* **11**(1), 7172 (2021).
- <sup>15</sup>F. Khan, W. Khan, J. H. Kim, N. U. Huda, H. M. Salman Ajmal, and S. Kim, *AIP Adv.* **8**(7), 75225 (2018).
- <sup>16</sup>H. So, J. Lim, and D. G. Senesky, *IEEE Sens. J.* **16**(10), 3633–3639 (2016).
- <sup>17</sup>Z. H. Zaidi and P. A. Houston, *IEEE Trans. Electron Devices* **60**(9), 2776–2781 (2013).
- <sup>18</sup>K. Zhou, L. Shan, Y. Zhang, D. Lu, Y. Ma, X. Chen, L. Luo, and C. Wu, *IEEE Electron Device Lett.* **44**(5), 781–784 (2023).
- <sup>19</sup>A. S. Razeen, D. Kotekar-Patil, E. X. Tang, G. Yuan, J. Ong, K. Radhakrishnan, and S. Tripathy, *Mater. Sci. Semicond. Process.* **173**, 108115 (2024).
- <sup>20</sup>K. Wang, X. Qiu, Z. Lv, Z. Song, and H. Jiang, *Photonics Res.* **10**(1), 111 (2022).
- <sup>21</sup>W. Li, Y. Wang, G. Gu, F. Ren, D. Zhou, W. Xu, D. Chen, R. Zhang, Y. Zheng, and H. Lu, *IEEE Trans. Electron Devices* **70**(7), 3468–3474 (2023).
- <sup>22</sup>Y. Li, Y. Liu, G. Yang, B. Bian, J. Wang, Y. Gu, Q. Fan, Y. Ding, X. Zhang, N. Lu, and G. Chen, *Opt. Express* **29**(4), 5466 (2021).
- <sup>23</sup>S. Shi, A. Zaslavsky, and D. Pacifici, *Appl. Phys. Lett.* **117**(25), 251105 (2020).
- <sup>24</sup>S. Kumar, A. S. Pratiyush, S. B. Dolmanan, S. Tripathy, R. Muralidharan, and D. N. Nath, *Appl. Phys. Lett.* **111**(25), 251103 (2017).
- <sup>25</sup>X. Tang, F. Ji, H. Wang, Z. Jin, H. Li, B. Li, and J. Wang, *Appl. Phys. Lett.* **119**(1), 13503 (2021).
- <sup>26</sup>L. X. Qian, H. Y. Liu, H. F. Zhang, Z. H. Wu, and W. L. Zhang, *Appl. Phys. Lett.* **114**(11), 113506 (2019).